

INTERIM REPORT

NASA GRANT NSG 1167

N76-78572

A COMPARISON BETWEEN EXPERIMENT AND THEORY FOR
A BORSIC-ALUMINUM PICTURE FRAME SHEAR TEST

Principal Investigator: M. W. Hyer
Assistant Professor of Engineering
Old Dominion University

Research Assistant: D.O. Douglas

Submitted by the: Old Dominion University Research
Foundation

Norfolk, Virginia 23508

(NASA-CR-148931) A COMPARISON BETWEEN
EXPERIMENT AND THEORY FOR A BORSIC-ALUMINUM
PICTURE FRAME SHEAR TEST (Old Dominion Univ.
Research Foundation) 20 p

N76-78572

Unclas
00/98 05337

July 23, 1976

Technical Monitor: John G. Davis, Jr.
Materials Division
Langley Research Center

INTRODUCTION

Picture frame shear tests are commonly used to determine shear strength and deformation characteristics of materials. If the frame is properly aligned, the specimen perfectly flat and the loads applied with no eccentricities, the specimen is subject to a state of pure shear. However, alignment problems, slight curvature in the panels, edge phenomenon and other uncontrollable effects always exist and the question arises as to how closely the situation compares with an ideal situation. Of particular interest is the purity of the shear and its uniformity over the specimen.

This investigation compares the experimental results of a picture frame shear test of a $\pm 45^\circ$ borsic aluminum/honeycomb sandwich panel with predictions obtained from an ideal situation as simulated by a finite element analysis using NASTRAN. Strains at several locations are used as a measure of comparison. Attention is given to the purity of the shear and its uniformity over the panel.

DESCRIPTION OF THE TEST

The experimental setup for a picture frame shear test is shown in Figure 1. The shear panel was bonded to a frame constructed from four 1 in. \times 1 in. (25.4 mm \times 25.4 mm) steel edge bars designed to simulate fully clamped edge conditions. The panel specimen was bolted to a test frame by 0.375 in. (9.52 mm) diameter bolts, seven per side. At each corner of the test frame loads were applied to the pin joints. Tensile loads were applied to the vertical pins and compressive loads were applied to the horizontal pins to produce the shear loading in the test specimen. The test specimens were made using 7 in. \times 7 in. (178 mm \times 178 mm) borsic aluminum sandwich shear panels. With the addition of 1 in. \times 1 in. (25.4 mm \times 25.4 mm) steel edge bars, the overall dimensions of

the shear panel were 9 in. \times 9 in. (229 mm \times 229 mm). To permit installation of the pins on the test frame, a portion of the shear panel was cut away at each corner. Each corner had a radius of 0.25 in. (6.35 mm). The test specimen is shown schematically in Figure 2.

The two face sheets of the sandwich panel were separated by a honeycomb core. On each face sheet there were four piles, each .0285 in. (.724 mm) thick, at a $\pm 45^\circ$ layup. The panel face sheets were cut from 10 in. (254 mm) square laminates. The filaments of the laminate were parallel or perpendicular to the applied loads. With the face sheets and honeycomb core, the panel was nominally 1 in. (25.4 mm) thick.

NASTRAN ANALYSIS

The shear panel was analyzed using quadrilateral and triangular membrane finite elements. The panel itself was represented with orthotropic elements while the steel edge bars were represented using isotropic elements. Any stiffness of the core was ignored and the load was applied through 7 points on the steel edge bars. Due to symmetry only $\frac{1}{4}$ of the panel was represented. Figure 3 shows the grid geometry, loading and boundary conditions. Further details of the analysis are available in reference 1. Elastic moduli data for the NASTRAN analysis was obtained from uniaxial tests reported on by Viswanathan, Herakovitch and Davis (ref. 2).

COMPARISON OF EXPERIMENTAL AND ANALYTICAL RESULTS

The comparison was done for experimental test 560, run 7. Figure 4 shows the location and numbering scheme for the strain gages and the direction of the applied load. The numbers in circles represent strain gages on the opposite face sheet. Thus gages 6 and 22, 7 and 21, 8 and 20, 14 and 17, 13 and 18, and 12 and 19 represent back-to-back gages. Ideally, the two gages in a back-to-back pair should

indicate identical strains. Rosettes 6-7-8 and 9-10-11 are symmetrically placed and should also measure identical strains. Although not exactly symmetric pairs, rosettes 12-13-14 and 3-4-5 should indicate similar strains. Uniformity of the shear strain was measured by the closeness of the shear strain values at the various locations. Gages 1 and 16, 7 and 15, and 23 and 24 represent other strain gages located symmetrically on the panel.

Figure 5 shows a plot of the applied load versus compressive strains at gages 6, 11, and 22. The plot shows both the NASTRAN predictions and the experimental results. The strains for these locations should be identical. As can be seen, the experimental strains are quite close to each other and in fair agreement with theory. However, gage 22 is subject to slightly larger values of compressive strains, indicating a slight bowing of the panel. Referring to Figure 4, the values of strain indicate the panel is bowing upward, out of the plane of the figure. Figure 6 shows a similar plot for compressive strains at gages 3, 14, and 17. Figure 7 shows compressive strain values for gages 2 and 15. The strain values are similar although the deviation of these symmetrically placed gages is larger than for previous sets. If the panel were in a state of pure shear, the compressive strains would be the same at all locations on the panel. However, both the NASTRAN analysis and the experiment indicate that along the diagonal of the panel the compressive strain is fairly consistent while off the diagonal the strain is larger. This is due to the edge effects of the steel bars.

Figure 8 shows theoretical and experimental extensional strains for gages 8, 9, and 20 and it is evident also from the strain values of these gages that the panel is bowed. Figure 9 shows similar plots for gages 5, 12, and 19. Plots for gage pairs 1 and 16 and 23 and 24 are indicated on Figures 10 and 11, respectively. Figures 8, 9, and 10 indicate, both experimentally and theoretically, that the elongation strains increase off the diagonals. Gages 23 and 24 are in a region of high stress gradients and, in addition,

the gage dimensions are the same order of magnitude as the radius of curvature of the corner cut-out. Thus it is not surprising that the comparison in this region is poor.

Figure 12 shows the shear strain at all rosette locations. Comparison of rosette pairs 6-7-8/9-10-11 and 3-4-5/12-13-14 indicate the shear is symmetrically distributed on the panel. Due to bowing of the panel, the shear is not the same on the top and bottom face sheets. In addition, both the theory and experiment indicate that the shear strain increases away from the center of the panel. Over the entire local range, the diagonal tension and compression loads were equal to within 1 percent.

For a state of pure shear, Mohr's circle of strain is centered at zero. In actual practice this is never achieved and a useful measure of the closeness to a state of pure shear is the ratio of the center of Mohr's circle to the radius, or, the eccentricity. The smaller the ratio, the closer the state of strain is to a state of pure shear. Table 1 shows the theoretical and values of eccentricity at the various rosette locations. The experimental values in the table are the maximum value of the ratio for a particular rosette over the entire local range of the test. The theoretical values of course are independent of load. Even though the experimental values of the eccentricity are an order of magnitude larger than theoretical values, the experimental eccentricity is small enough to assume that shear deformation dominates.

Assuming a state of uniform shear over the panel, the shear modulus computed using the strain at the center of the panel is 5.19×10^6 psi (3.58×10^{10} pascals).

CONCLUSIONS

Overall the comparison between experiment and theory was quite reasonable. Bending effects prevented the top and bottom panel from having the same load

condition. Results indicate that due to the small panel size and edge effects, a state of pure, uniform shear is not possible with this type of experimental configuration. Both the experimental results and NASTRAN results indicate that the strains increase away from the center of the panel but the state of strain is quite close to a state of pure shear as evidenced by the low eccentricity to Mohr's circle of strain. Future shear tests, of all types, could compute the eccentricity to determine the degree of shear strain occurring.

REFERENCES

1. Douglas, D.O., Holzmacher, D.E., Lane, Z.C., and Thornton, E.A.: Studies in Finite Element Analysis of Composite Materials. Old Dominion University School of Engineering Technical Report 75-M3, pp. 1-24.
2. Viswanathan, C.N., Davis, John G., Jr., and Herakovich, Carl T.: Tensile and Compressive Behavior of Borsic/Aluminum Composite Laminates. VPI Report VPI-E-75-12, p. 26.

Table 1. Experimental and Theoretical Values
of Eccentricity of Mohr's Circle of
Strain.

Rosette	Theoretical (%)	Experimental (%)
3-4-5	2.8	7.6
6-7-8	.9	9.0
9-10-11	.9	11.0
12-13-14	2.8	6.2
17-18-19	2.8	12.0
20-21-22	.9	13.0

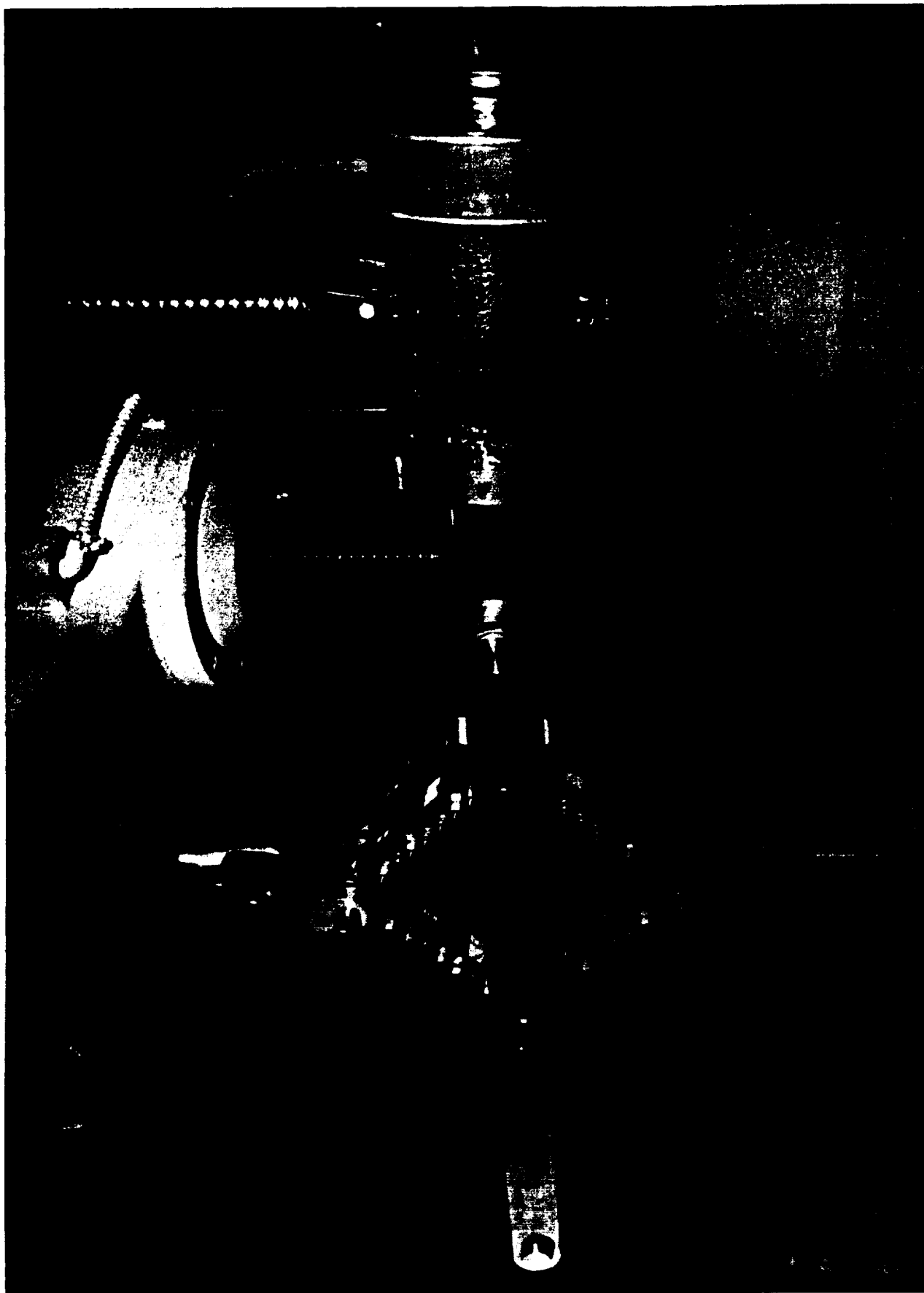


Figure 1. Picture Frame Shear Test Experimental Setup at Langley Research Center.

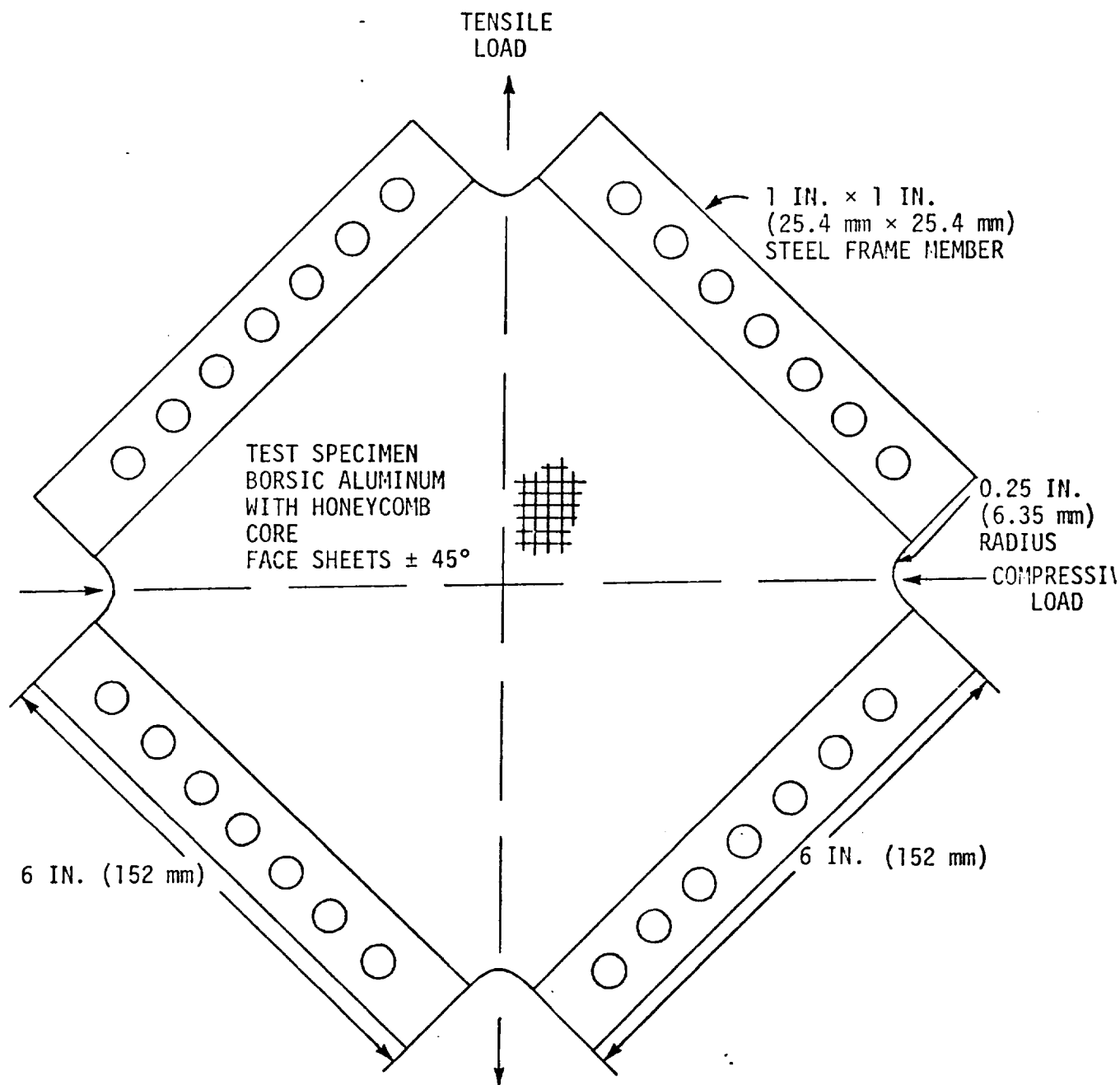


Figure 2. Schematic of Test Specimen.

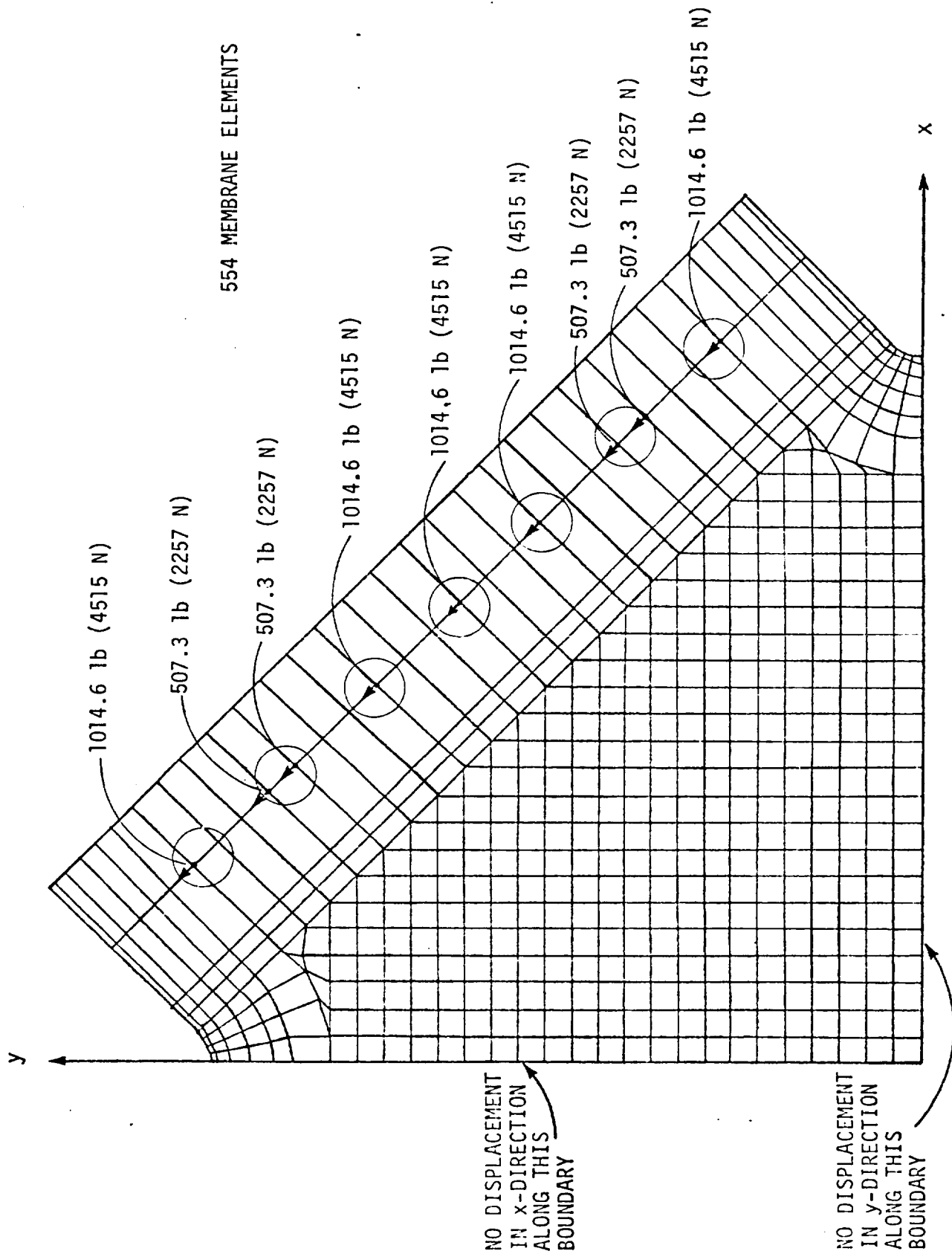


Figure 3. Finite Element Model of Shear Panel.

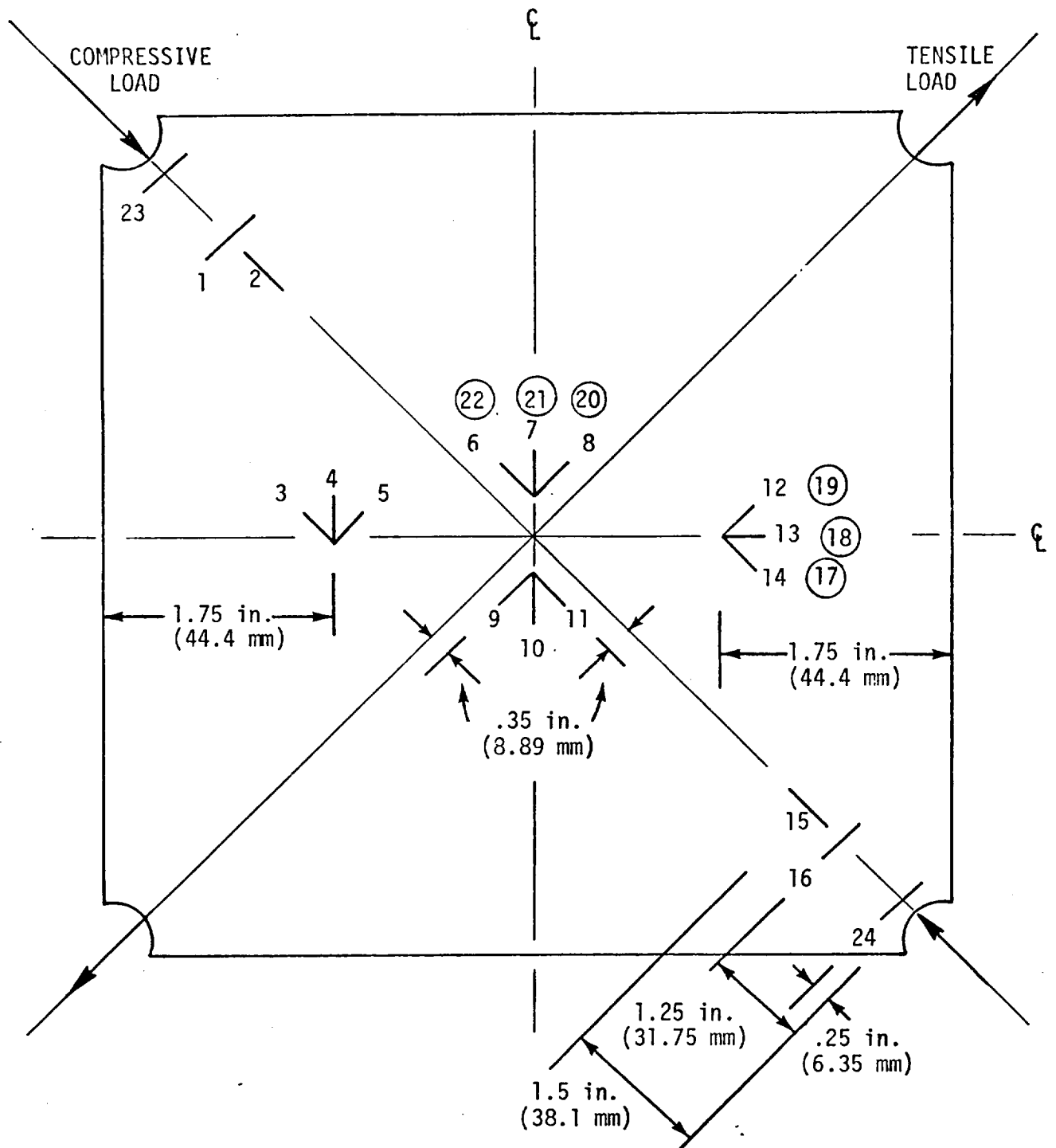


Figure 4. Strain Gage Location.

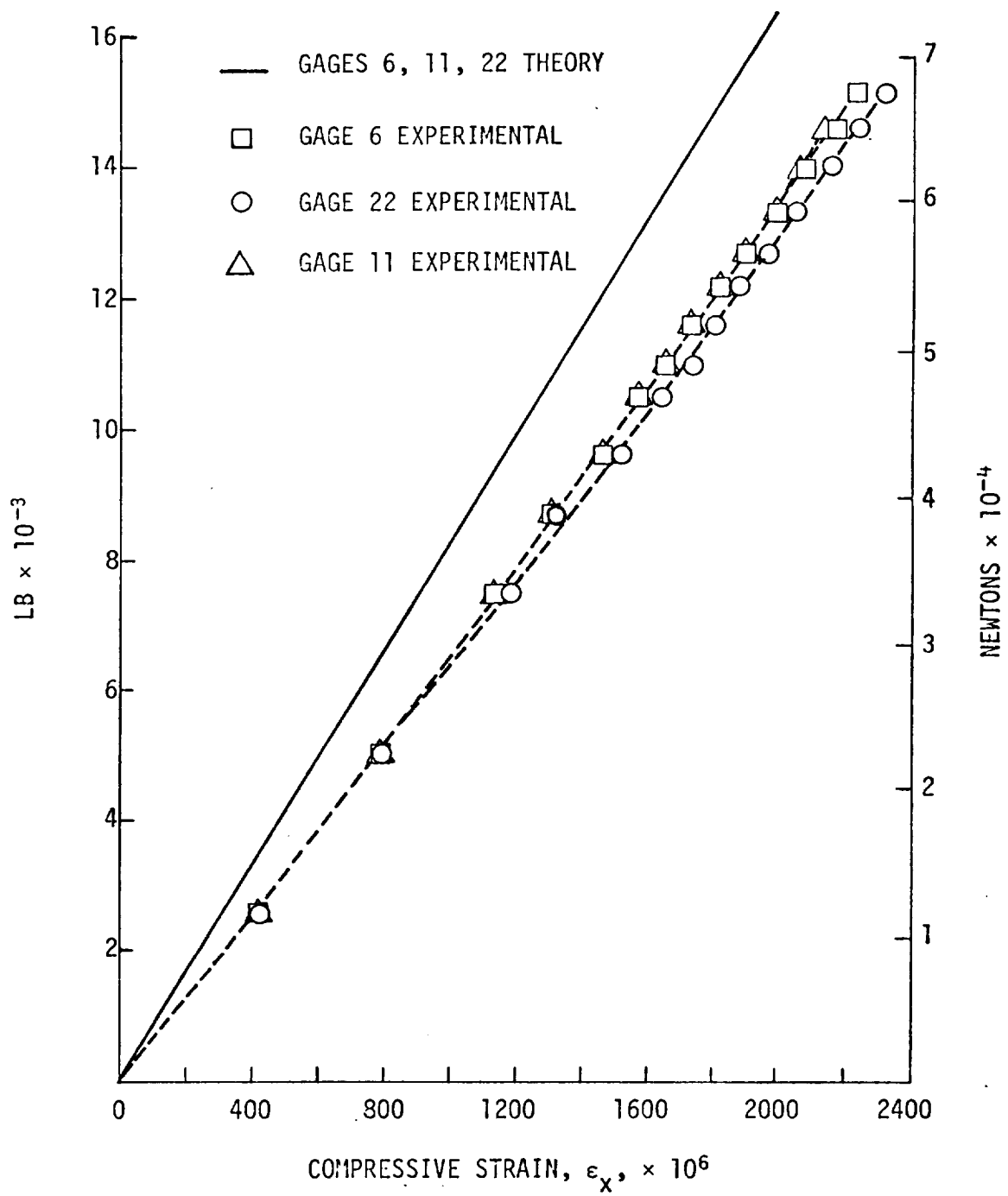


Figure 5. Applied Load vs. Strain in Gages 6, 11 and 22.

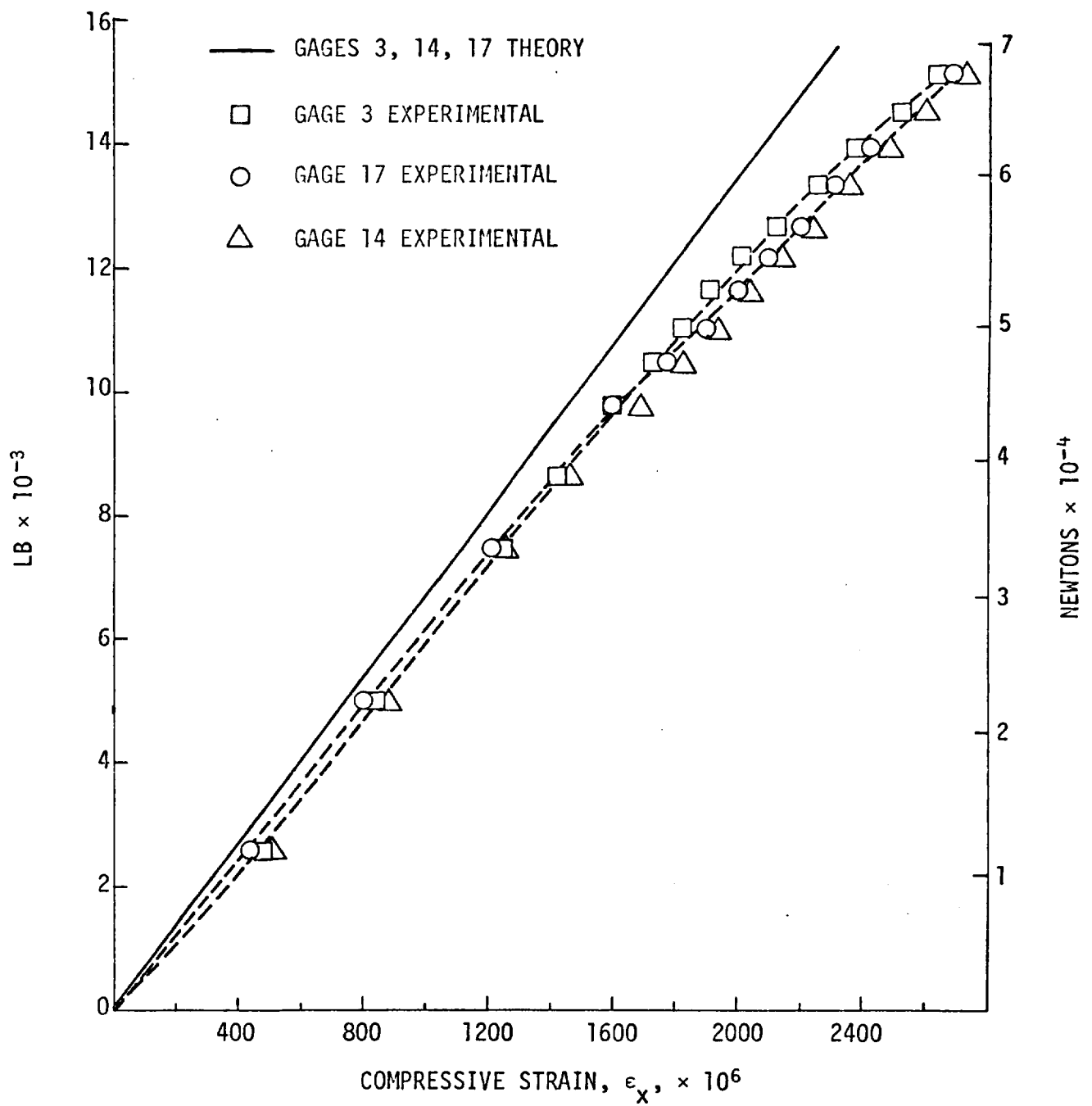


Figure 6. Applied Load vs. Strain in Gages 3, 14 and 17.

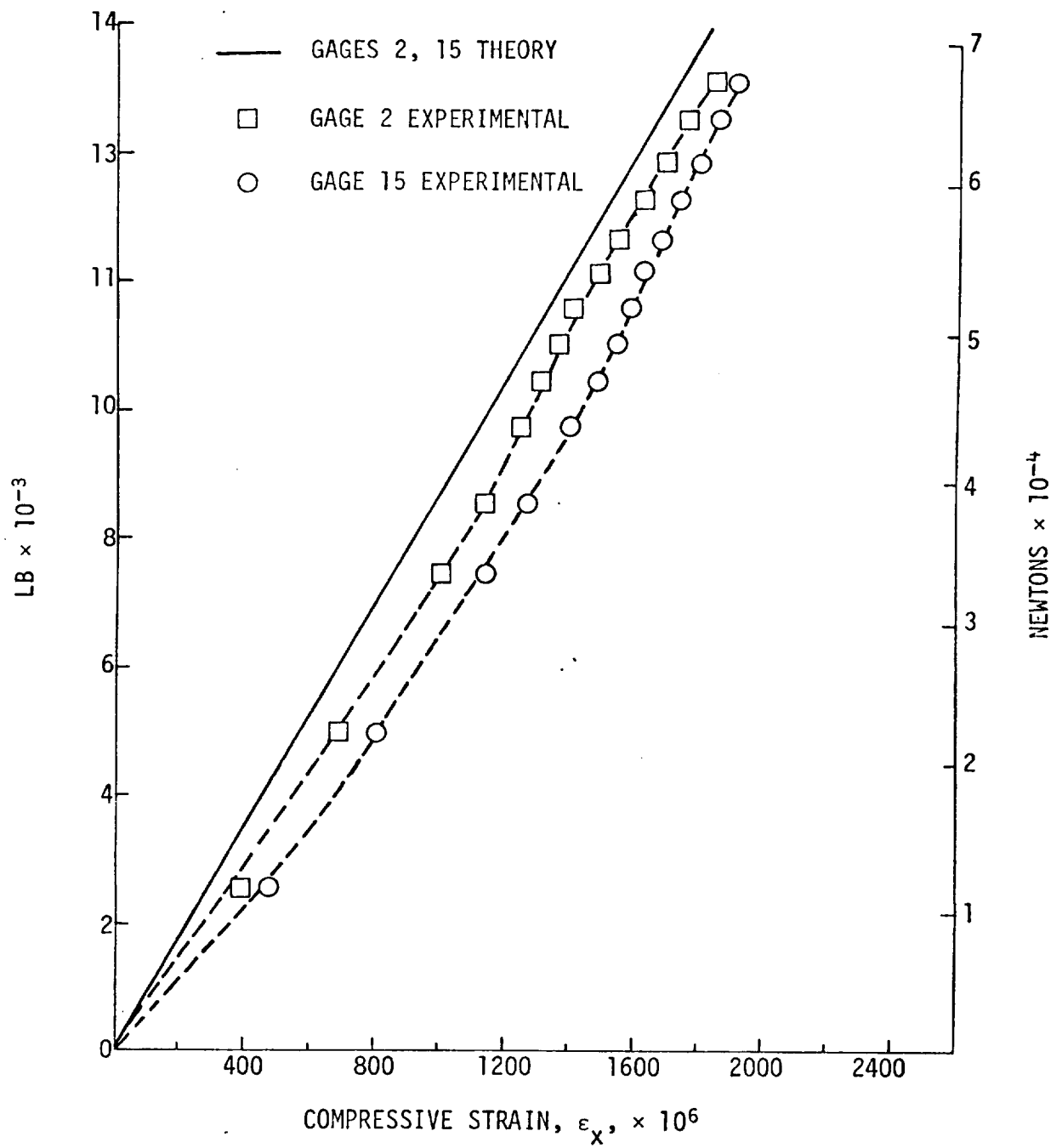


Figure 7. Applied Load vs. Strain in Gages 2 and 15.

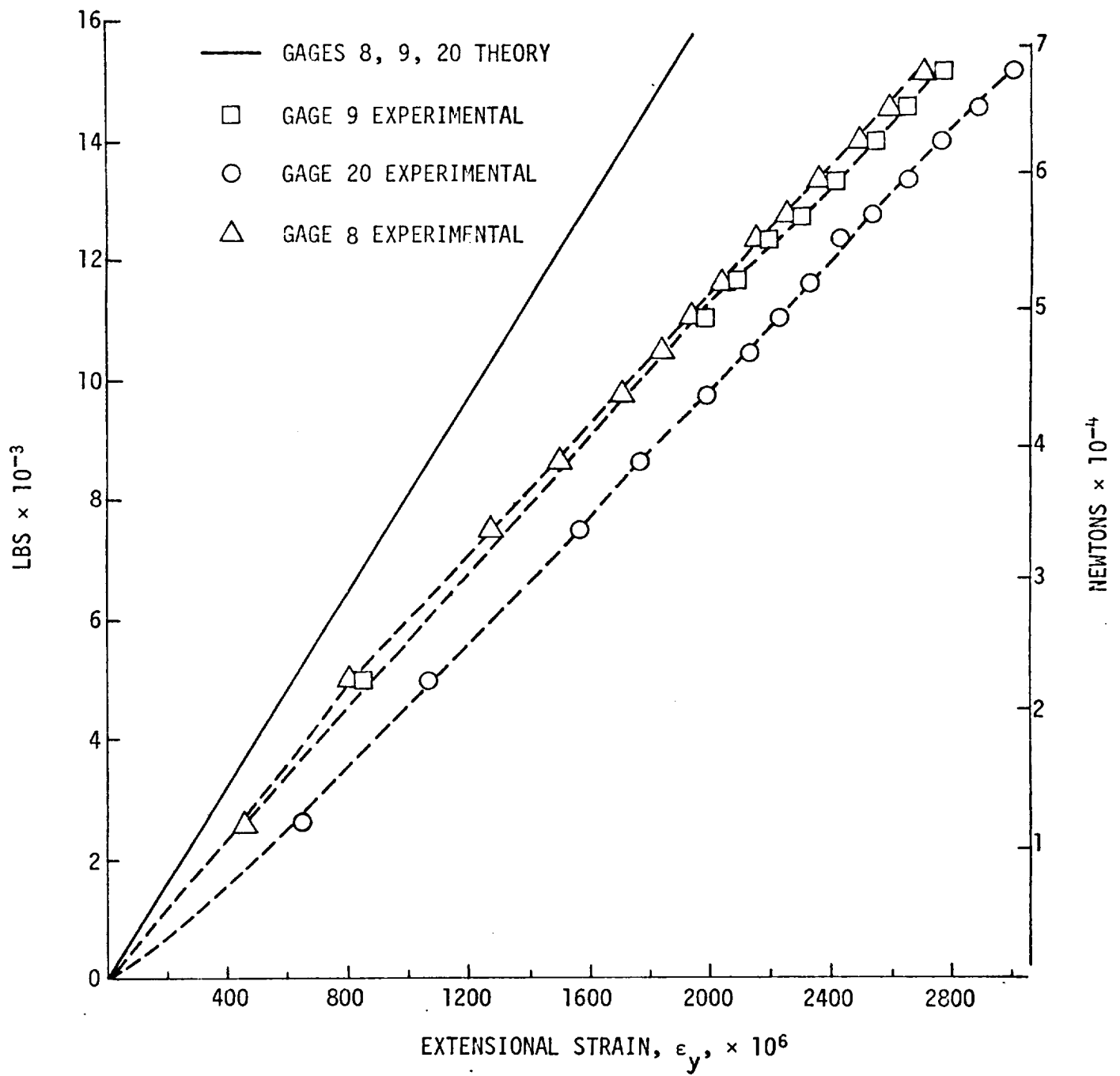


Figure 8. Applied Load vs. Strain in Gages 8, 9 and 20.

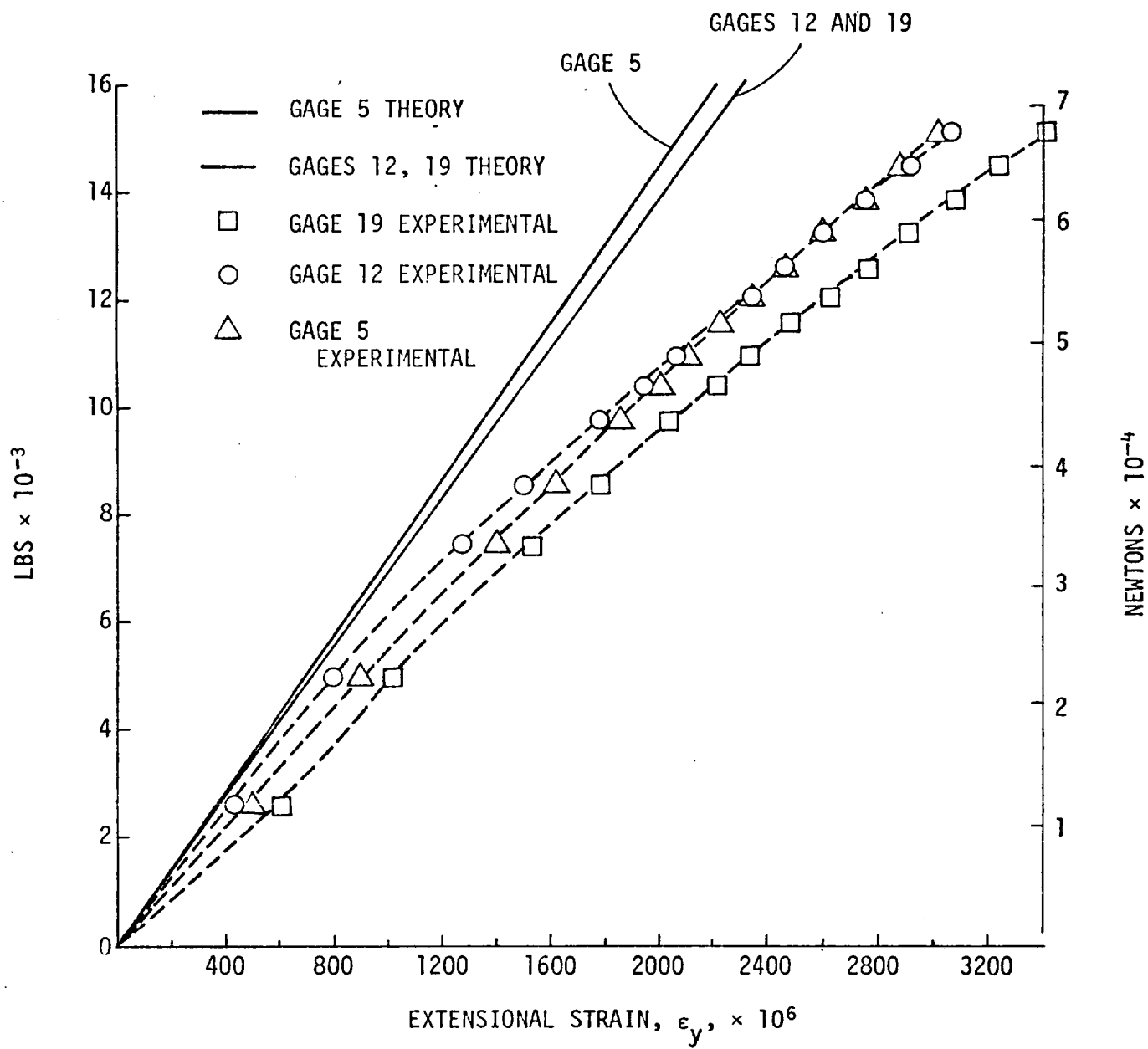


Figure 9. Applied Load vs. Strain in Gages 5, 12, and 19.

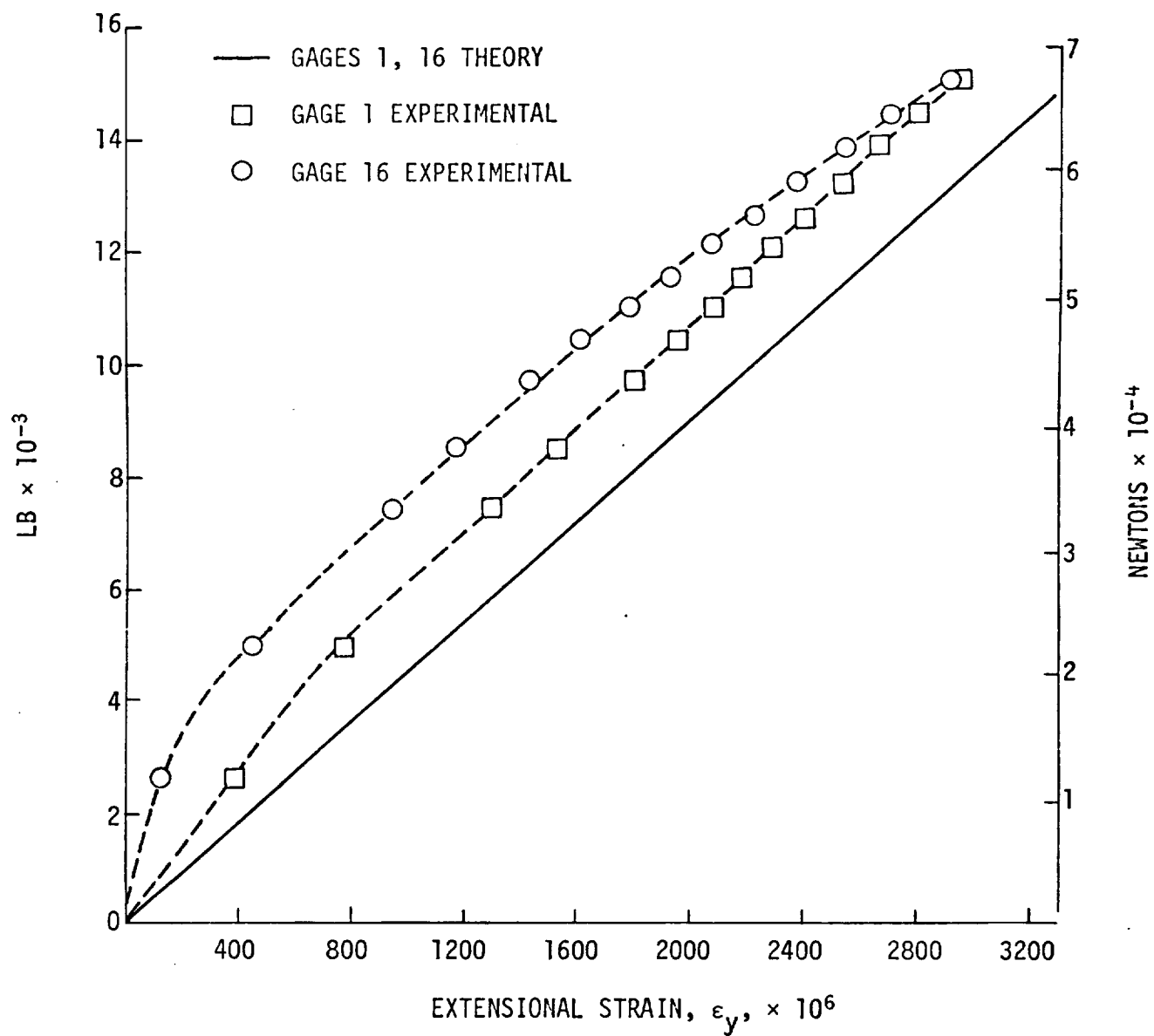


Figure 10. Applied Load vs. Strain at Gages 1 and 16.

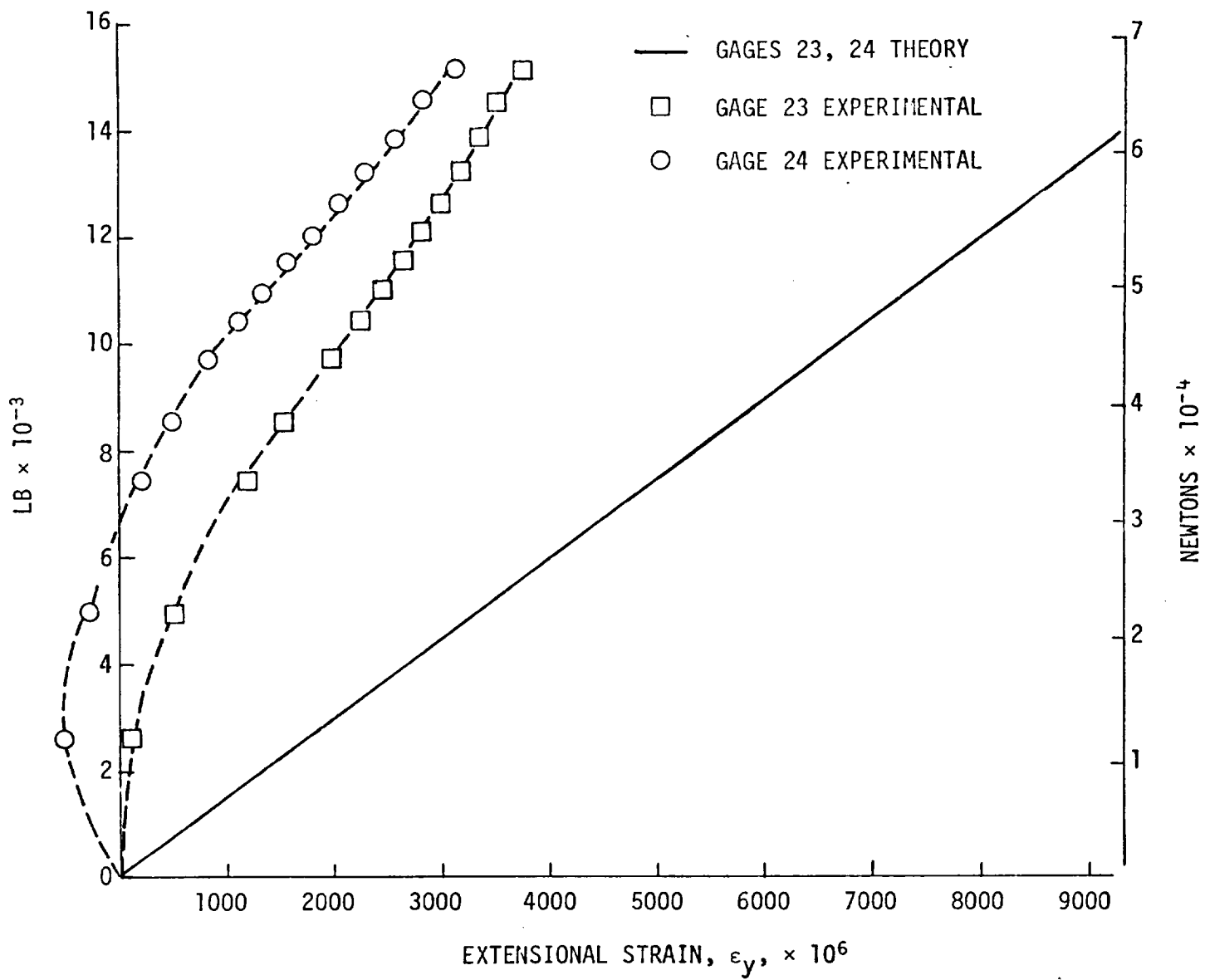


Figure 11. Applied Load vs. Strain in Gages 23 and 24.

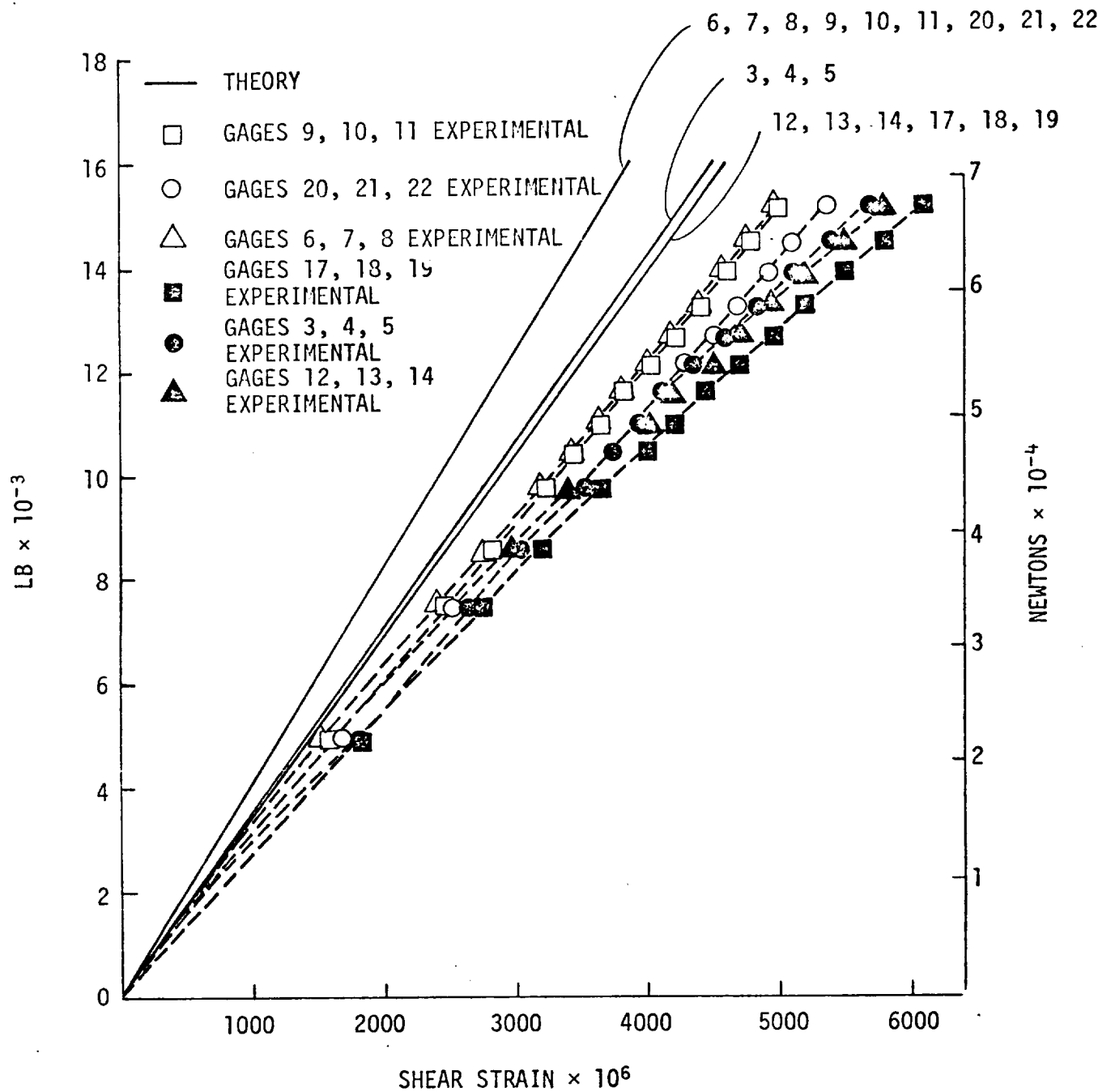


Figure 12, Applied Load vs, Strain at Rosette Locations,